Eco. Env. & Cons. 27 (October Suppl. Issue) : 2021; pp. (S25-S32)
Copyright@ EM International
ISSN 0971–765X

Temporal monitoring of Algae Blooms in a Drinking water reservoir using Landsat-8 Oli Data

Haidi Abdullah[1,2] and Tarq K. Hassan[1]

[1]Department of Geography, College of Arts, Salahaddin University-Erbil, Iraq
[2] Vultus AB, Lilla Fiskaregatan 19, 222 22, Lund, Sweden

(Received 3 January, 2021; accepted 26 January, 2021)

ABSTRACT

Algal blooms in drinking water reservoirs present a major natural concern around the world, coming about in water contamination, expanded water treatment costs, and dangers to human and creature wellbeing. Conventional observing approaches utilizing ship-based strategies that incorporate field examining and research facility examination are exceptionally difficult, expensive, wasteful, and troublesome to apply for administration purposes in large water bodies. The use of satellite technology can pre-empt such limitations. Here we show that Landsat-8 Operational Land Imager (OLI) time-series imagery has a great protentional to provide valuable spatiotemporal information regarding surface algae blooms. We calculated the surface algae bloom index (SABI) and utilized meteorological data (air temperature, solar radiation, total water runoff and precipitation) to monitor algae blooms from January until December 2019. The results show severe algae blooms during summer months (June, July, and August). Furthermore, we observed a high positive correlation (r = 0.77) between solar radiation and SABI value, indicating SABI's sensitivity for detecting surface algae blooms. The results of this study demonstrate the enormous potential of Landsat-8 OLI data as additional monitoring tools for Lake Dukan resource managers.

Key words *: Landsat-8 OLI, Time series data, Algae blooms, Surface Algae Bloom Index*

Introduction

Water quality and quantity are critical components of global freshwater security and ecosystem health (Cook and Bakker, 2012). The term water quality was created to indicate the suitability of a water source for human consumption (Vaux, 2001). In many middle and low-income countries, poor water quality is one of the largest societal problems. Therefore, the Sustainable Development Goals (SDGs) program of the United Nations (UN) has prioritized access to clean water and sanitation as Goal 6 (Setty, Jiménez *et al*., 2020). In recent decades, research advances have allowed for the collection of more consistent and accurate information on inland water quality in different parts of the world. They accomplished this by focusing on multiple physical, chemical, and biological factors that can determine the quality of water in any aquatic ecosystem. One of the most common approaches to assessing water quality in inland water bodies is monitoring harmful algae blooms, an enormous concern for environmental and public health managers (Chorus and Bartram, 1999). In general, algae play an important role in assessing the quality of the water system. Algae species are significant indicators of the water environment since they respond- in terms of species composition - qualitatively and quantitatively to a wide range of water quality types. This response is due to changes in water chemistry, such as increased

contamination by different types of wastes which may be tolerated by only some species. The impacts of the harmful algae blooms can vary, ranging from simple aesthetic issues related to colour, taste, and odour, to the production of dangerous toxins (Codd, Lindsay *et al*., 2005). As a result, continuous monitoring of algal blooms is critical to adjust treatment methods appropriately, especially in those bodies used for drinking water.

Conventional algal bloom monitoring as a rule requires field studies and ship-board field testing programs to collect water samples and determine algae concentrations, which incorporates estimation of chlorophyll a (chl-a), a photosynthetic colour utilized as a intermediary to measure algal biomass. This method is based on the collection of field samples. Therefore, it is very laborious, costly, and inefficient, and the results are challenging to apply for management purposes in large water bodies. Furthermore, due to the spatial and temporal heterogeneity of water bodies, the characterization of algal blooms is usually inadequate since it relies on interpolation and extrapolation among the sampled points (Ogashawara, Li *et al*., 2016).

Compared to the traditional field monitoring approach, remote sensing has great potential by providing regular, synoptic coverage over large areas in relatively short periods and Furthermore, remote sensing models can be utilized and developed to monitor algae blooms over a large area and in those areas that might otherwise be inaccessible.

Remotely sensed data depend on spectral signatures collecting over different regions in the electromagnetic spectrum. Unique spectral signatures have been used to derive (chl-a) concentrations as a proxy for monitoring algae blooms (Schalles, Gitelson *et al*., 1998; Keith 2010). Chl-a has a reflectance peak in the near-infrared (NIR) region. Therefore, for many algae species, chl-a is the preferred pigment to monitor phytoplankton blooms. This is because the NIR spectral band is provided by many satellite platforms, in particular, Landsat and Sentinel-2.

It is important to note that different types of phytoplankton blooms are disposed to different degrees of change over space and time. For example, one of the most widely blooming algae in the inland water bodies is cyanobacteria, which blooms on the water's surface. These algae are unequivocally influenced by some natural factors such as, temperature, wind and solar radiation during the day time; within a few days, a gigantic bloom can show up and totally vanish from the surface (Paerl, 1996; Hu, Lee *et al*., 2010). Some species of cyanobacteria are known to produce toxins and are harmful to both humans and those organisms living in the affected water body. As a result, the cyanobacteria are of particular interest to limnologists and lake users.

To protect and manage natural ecosystems affected by cyanobacteria blooms, timely and accurate monitoring is required (Bresciani, Giardino et al. 2017). Remote sensing is a valuable source that can provide sufficient data to monitor and detect different types of algae blooms in freshwater ecosystems (Hestir, Brando et al. 2015). In recent years, researchers have developed different algorithms to monitor multiple types of algae blooms utilizing remote sensing data .

The objective of this study was to use spectral data generated by the Landsat-8 OLI sensor to monitor algal blooms in the Dukan Lake drinking water reservoir (Figure 1). The lake is located in the northern part of Iraq and contains the oldest dam constructed in the area. The dam was built in 1959 to collect precipitation water for irrigation, generating electricity, and serving drinking water to the main cities and districts around the lake. In the last three decades, due to the dramatic decrease in rainfall during the rainy season, the amount of water collected by this dam has decreased, and its water quality changed (Pilesjo and Al-Juboori, 2016). For this purpose, the main aims of this study were to (1) retrieve atmospherically corrected spectral reflectance signatures from Landsat-8 OLI over the entire year to identify and understand the most sensitive spectral region for monitoring algae blooms in this lake, (2) calculate the spectral index to map temporal variation of algae blooms during the entire year and (3) explore the correlation between remote sensing data with meteorological data in regards to algae blooms.

Methods and Materials

Study site and meteorological data

The study site is Dukan Lake, located 63 km northwest of the city Sulaymaniyah and approximately 133 km from the city of Kirkuk and 300 km from Baghdad, northern Iraq, between longitude 44°55'E , and latitude 36°08'N. (Fig.1). The elevation in this region ranges from 1230 m to 1860 m. This region is characterized by a Mediterranean climate with total

annual precipitation between 600 and 760 mm and a yearly mean temperature between 5.7 and 32.9 °C. The lake formed as a result of the construction of Dukan Dam in 1959, an arched reinforced concrete barrier with a height of 115.6 m (Toma, 2019). The dam interrupts the course of the lower Zab River (Little Zab) at the strait, forming a very large reservoir. The reservoir holds up to 5.2 billion m^3 of water. The surface area is 221 km^2 in the flood season and 12 km^2 at other times of the year.

The meteorological data were obtained from Dukan observational station. The station is built at an elevation of 800 m above sea level and the location was strategically placed to observe the different climatological and landscape types. Data on the monthly average air temperature, precipitation (mm), solar radiance (W/m^2) and total runoff per month (mm) were collected

Satellite imagery

In this study, cloud-free images (on-demand production) of Landsat 8 Operational Land Imager/Thermal Infrared Sensor (OLI/TIRS) surface reflectance data were downloaded from the USGS Global Visualization Viewer (http://glovis.usgs.gov/). The on-demand product is atmospherically corrected and the digital value converted to surface reflectance. Landsat-8 has two sensors called Operational Land Imager (OLI) and Thermal Infrared Sensor (TIRS). The OLI sensor collects data over the optical spectral region ranging from 0.43–2.29 nm with a 30 m spatial resolution, and the TIRS sensor collects data over thermal infrared region ranging from 10.6–12.5 nm with a 100 m spatial resolution resampled to 30 m in the delivered data product. Twelve images were selected for January until December 2019 (Table 1). The chosen images were des-

Table 1. List of Landsat-8 OLI images used in this study.

No	Acquisition date (dd/mm/yyyy)	Image ID
1	23-01-2019	LC08169035201901 2301T1-SC20200827150740
2	24-02-2019	LC08169035201902 2401T1-SC20200827150836
3	25-03-2019	LC08169035201903 2501T1-SC20200827151337
4	22-04-2019	LC08169035201904 2201T1-SC20200827150739
5	24-05-2019	LC08169035201905 2401T1-SC20200827150720
6	25-06-2019	LC08169035201906 2501T1-SC20200827150820
7	18-07-2019	LC08169035201907 1801T1-SC20200827150737
8	19-08-2019	LC08169035201908 1901T1-SC20200827150631
9	20-09-2019	LC08169035201909 2001T1-SC20200827151250
10	18-10-2019	LC08168035201910 1801T1-SC20200828081426
11	15-11-2019	LC08169035201911 1501T1-SC20200827150743
12	18-12-2019	LC08168035201912 1801T1-SC20200827151257

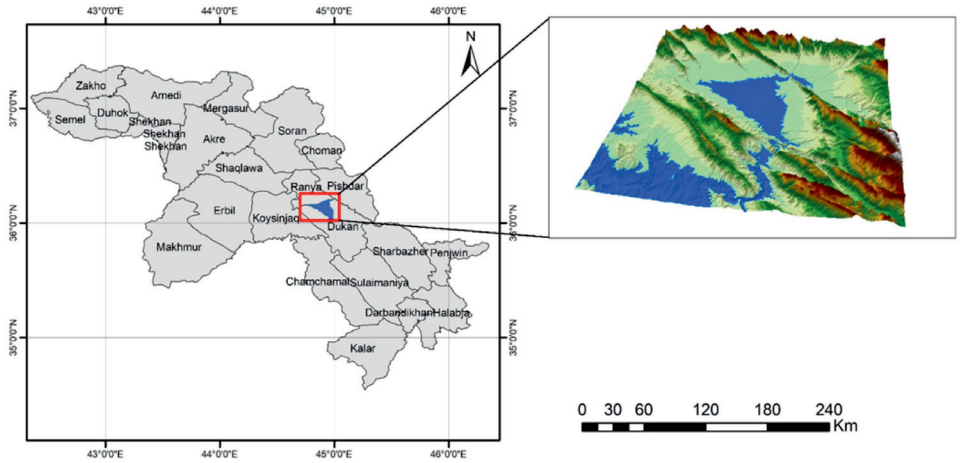

Fig. 1. Location of the study site in northern Iraq.

ignated to cover the entire year and all seasonal variation

Spectral index

Several spectral vegetation indices exist in the literature for monitoring and detecting different types of algae blooms (Klemas, 2012). This study selected the surface algal bloom index (SABI) developed by Alawadi (2010). The SABI was developed to detect biomass floating on water that has a spectral reflectance signature in the near-infrared spectral region, similar to that of land vegetation. Furthermore, the SABI utilizes the blue band in the visible region as it is sensitive to the specific inclusion of ocean (characteristic of clear water) and green band (characteristic of the water column bloom). This algorithm was particularly demonstrated to adapt to the marine habitat through its incorporation of sensitive water colour bands in a four-band ratio-based relationship. The algorithm has demonstrated high stability against various environmental conditions such as aerosol and sun glint. The mathematical transformation for computing the SABI is provided below

$$\text{SABI} = \frac{\text{NIR} - \text{RED}}{\text{Blue} + \text{Green}}$$

in which NIR is near-infrared spectral band ranges between 0.85–0.88 micrometre, and red, blue and green are spectral bands within the visible spectral region ranges from 0.45–0.67 for Landsat-8 OLI data.

Data Analysis

Two statistical analyses were utilized. First, to investigate the relationship between the measured SABI and the data collected from the weather station (air temperature, precipitation, runoff, and solar radiation), Pearson's correlation coefficients were calculated. Second, to understand the temporal variations of Landsat-8 OLI spectral bands for all images considered in this study, a box plot technique was utilized to investigate the spectral, temporal variation.

To generate the map of algae blooms, we utilized the calculated SABI maps. First, the SABI value was normalized between 0 and 1 using the MinMax normalization method as follows

$$\text{Normalized SABI} = \frac{X - Xa}{Xb + Xa}$$

in which X is the SABI value, and Xa and Xb are the minimum and maximum values, respectively.

Finally, to generate the algae bloom map, specific criteria were applied to classify the calculated normalized SABI maps for each image considered in this study (Table 2). The final map contains four classes corresponding to the level of algae bloom in each month.

Table 2. Algae bloom level categories are classified using the calculated normalized SABI values

No	Bloom level	Normalized SABI value
1	No bloom	0 – 0.3
2	Low bloom	0.3 – 0.5
3	Moderate bloom	0.5 – 0.7
4	Severe bloom	0.7 – 1

Results

Temporal variation of measured meteorological data

The monthly trend based on air temperature, precipitation, total runoff, and solar radiation is presented in Fig. 2. As can be seen from Fig. 2 A and B, the mean air temperature and solar radiation were similar low during the cooler months (January, February, November and December) and high during the warmer months (June, July and August). Furthermore, both total precipitation and total runoff followed a similar pattern for January, February, March and April. However, they showed a different pattern for October, November and December as the total precipitation increased after the dry period, whereas the trend of total runoff did not significantly change (Fig. 2 C and D)

Correlation between SABI and measured meteorological data

Pearson's correlation coefficients were calculated to explore the relationship between calculated SABI and measured meteorological data (air temperature, precipitation, total runoff and solar radiation). As shown in Fig. 3, for both air temperature and solar radiation (green dots) strong positive correlation observed with SABI (r = 0.71 and 0.78), respectively. On the other hand, a high negative correlation was observed between total rain and total runoff (red dots) with SABI values of r = -0.66 and -0.61, respectively

Temporal variation of Landsat-8 OLI spectral data and mapping algae blooms

We assessed surface water reflectance response to

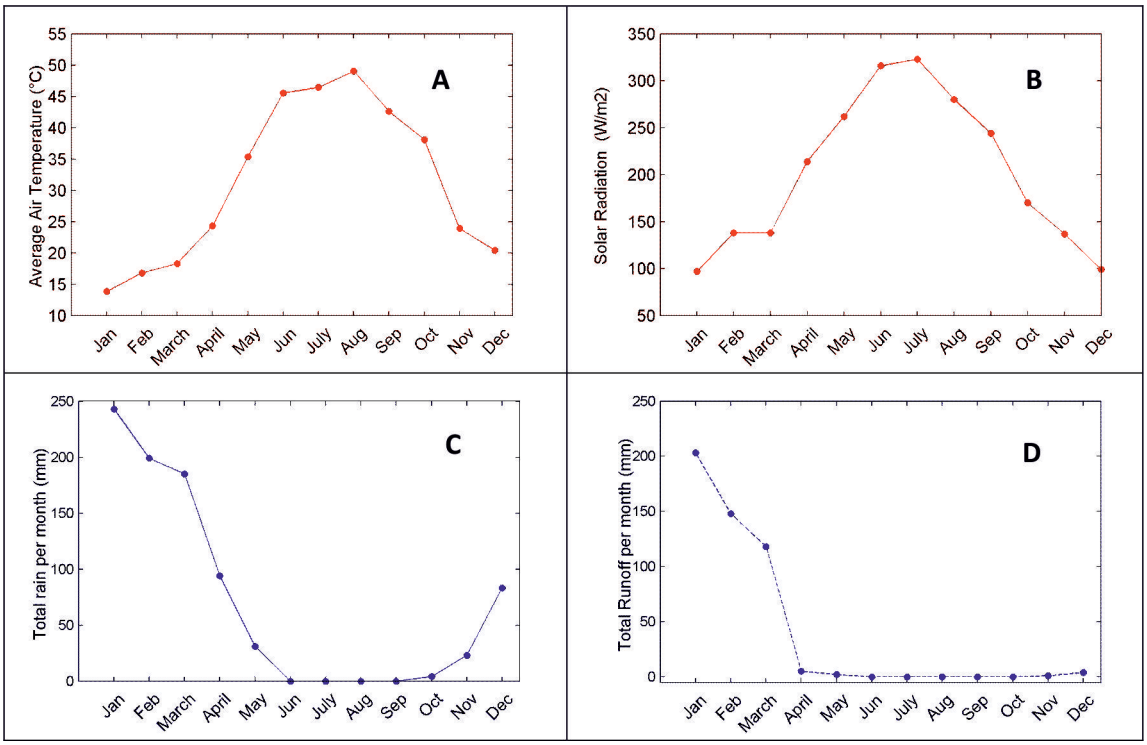

Fig. 2. The trend of monthly based, air temperature (A), solar radiation (B), total rain per month (C), and total runoff (D).

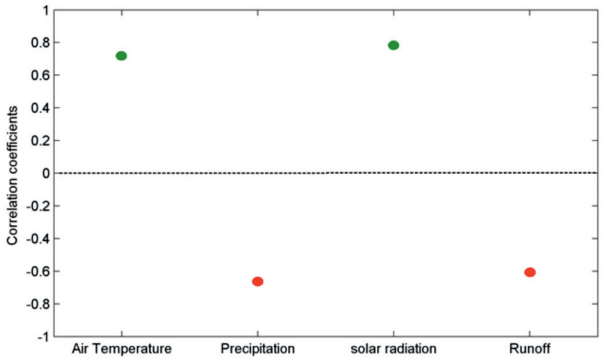

Fig. 3. Correlation between SABI index and metrological data (air temperature, precipitation, totalrunoff and solar radiation). Red dots indicate negative correlation and green dots indicates positive correlation

an algae bloom, employing a time series of Landsat-8 OLI images. The reflectance data were collected from each image, and for the entire lake, we studied the boxplots for all spectral bands and all months considered in this study. Figure 4 shows a comparative time-series of Landsat-8 OLI spectral bands over Dukan Lake. A symmetrical change of reflectance data was observed for all spectral bands obtained from Landsat-8 OLI. For example, all three spectral bands within the visible region (red, green, and blue) recorded similar spectral changes in May and June in summer, and November and December, in winter. Moreover, similar findings were observed for the spectral bands in NIR, SWIR 1&2, in particular in May and Jun (Fig. 4).

The defined threshold value of SABI (Table 2) was utilized to generate algae bloom maps for all 12 months. As shown (Fig. 5) in January, February, March, November and December, no algae blooms were observed over the study area. However, beginning in April, the severity of algae blooms increased, reaching its peak in August and decreasing again in September and October.

Discussion and Conclusion

In the present study, we explored the potential of the SABI index calculated from Landsat-8 OLI spectral data to monitor the temporal variation of algae blooms in Dukan Lake. The results confirmed the ability of Landsat-8 spectral data to detect subtle

changes in surface water reflectance due to algae blooms. Furthermore, the results of this study revealed that there is a strong positive correlation between the SABI value and air temperature and solar radiation.

All six spectral bands of Landsat-8 OLI used in this study, when implemented as a time series based on monthly images, showed distinct temporal variation in reflectance values, especially from April until August (Fig. 4). For example, both green and NIR spectral bands were more sensitive than the other spectral bands due to the increase in algae distribution over the lake surface (Fig. 5). The significant reflectance differences observed for green and NIR spectral bands might be due to backscatter from suspended sediments and floating algae over the lake surface (Doxaran, Froidefond *et al.,* 2002). Furthermore, it is well known that phytoplankton efficiency in inland water bodies is regularly gathered from the shape of visible spectra observed by earth-orbiting sensors. Therefore, more spectral variation will be observed within the visible spectral region.

In addition to the temporal variation, we also observed a strong correlation between meteorological data and the calculated SABI. For example, during the hot months of the year from May until August, when the air temperature and solar radiation increased, we observed high SABI (Fig.2 and 5). These

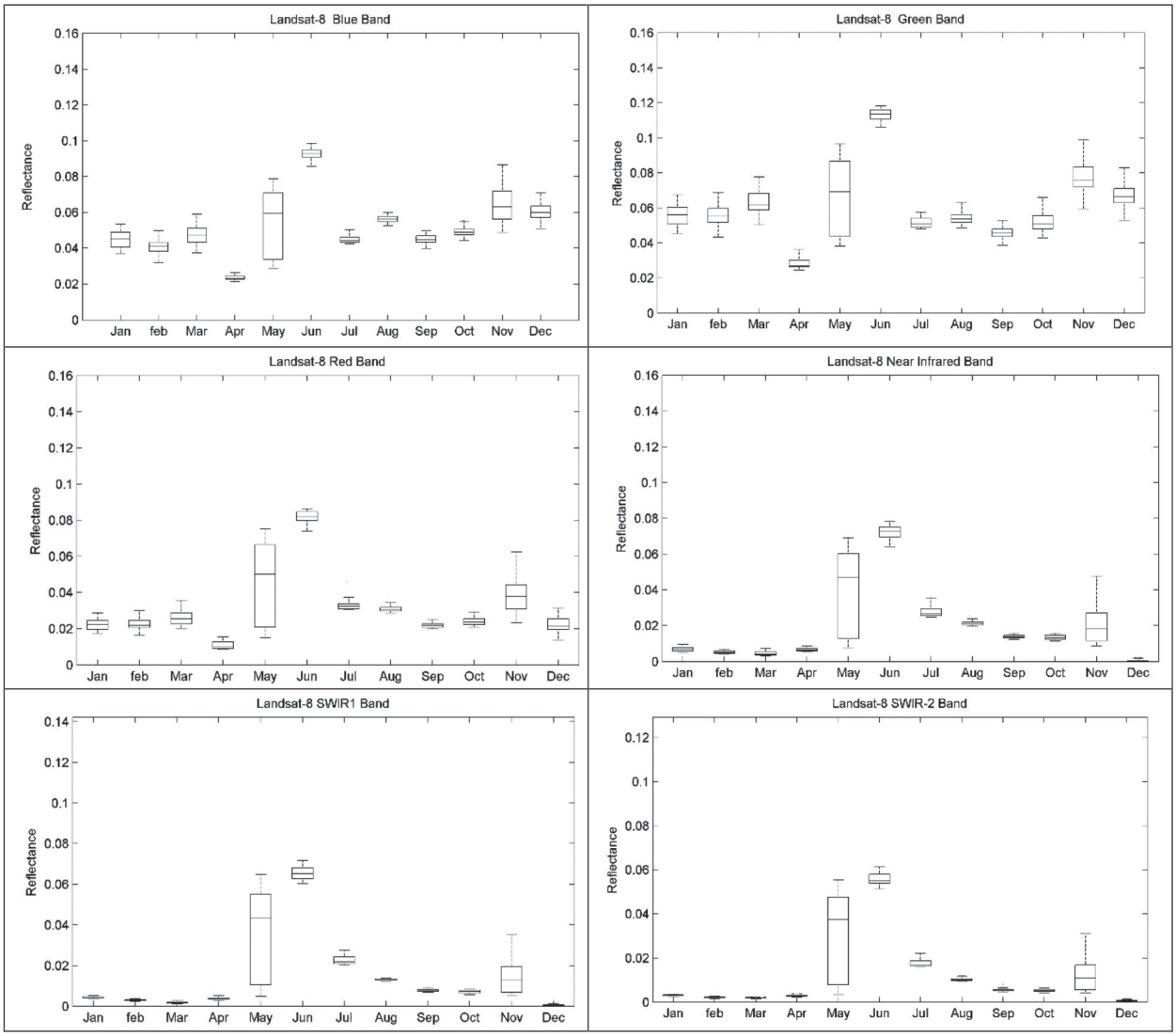

Fig. 4. Temporal variation of reflectance spectra over Dukan lake in the northern part of Iraq using Landsat-8 OLI satellite data.

results are consistent with previous findings by Reynolds (1990), who found that during the summer months (June, July, and August) different algae such as Ceratium hirundinella and Peridinium cinctum dominate and bloom in Dukan Lake. Algae blooms, including harmful algae, usually occur during the warm summer season or when water temperatures are warmer than usual (Toma, 2019). All types of algae blooming on the water surface observe sunlight (solar radiation) and make water even warmer to promote algae blooms. In general, when the water temperature rises, it will reduce and prevent the process of water mixing, leading to growing thicker algae in a faster way.

Similarly, during the rainy season from January until April, a strong negative correlation was observed between rainfall and total runoff with SABI value (Fig 3). These results can be attributed to the lakes' hydrodynamics and increased turbulence that perturb the calm environment for blooming algae (Vincent, Whyte *et al.,* 2009). Notably, the lake receives a high amount of water from the river's streams around the lake and melting snows during this period. For this reason, no algae bloom was observed during this period of the year (Fig. 5). In most cases, the dam administration will let water flow when the dam is reaching its capacity during this period of the year. In 2019, heavy rain caused more

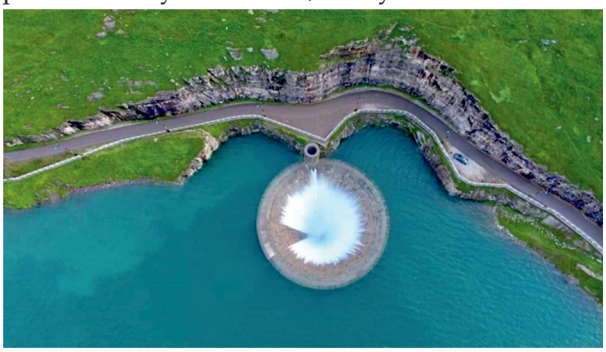

Fig. 6. A view of Dukan Lake bell-mouth spillway in 2019

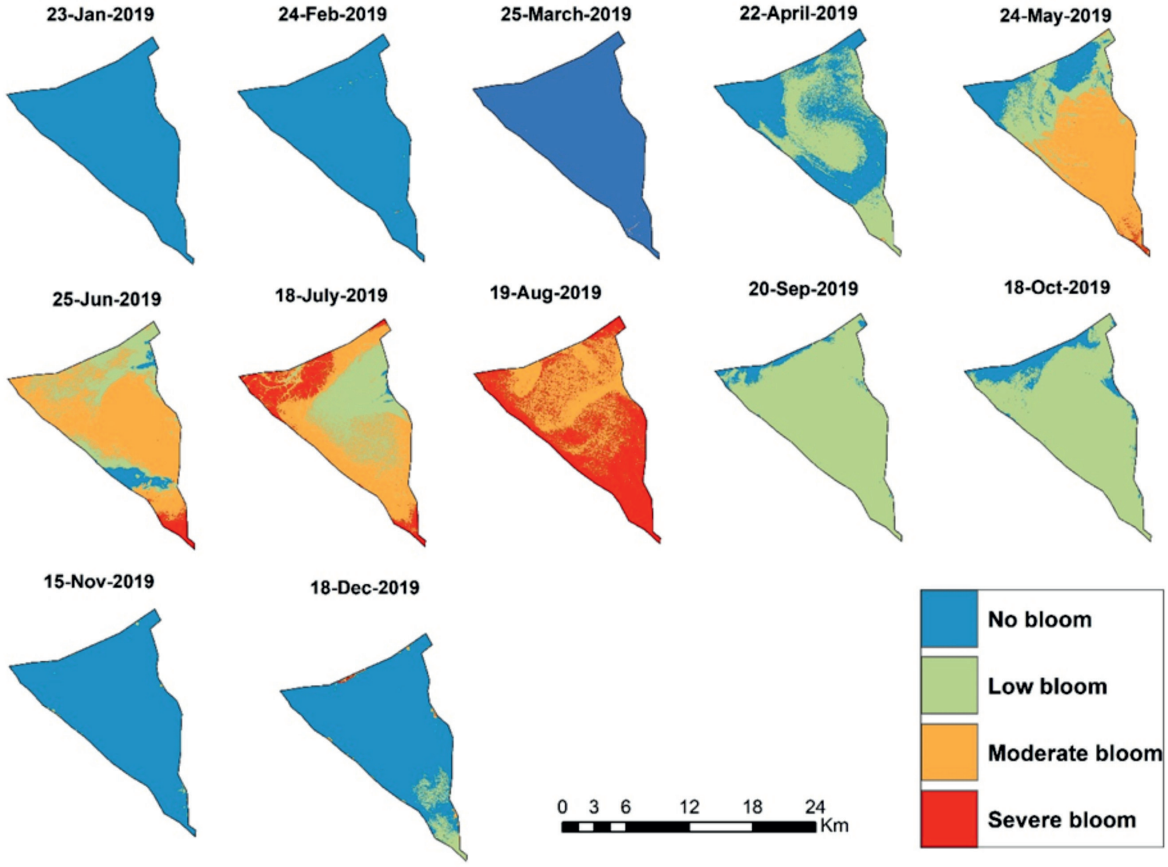

Fig. 5. Maps of temporal variation of algae bloom in Dukan lake, using SABI index calculated from Landsat-8 OLI satellite data

water to drain into the lake, and rivers flowing from the northeast were heavily draining into the lake, to entering through the bell-mouth spillway to help prevent floods from 'dam'-ageing or destroying a dam (Fig. 6).

These results confirm the importance of remotely sensed data to monitor the spatial and temporal frequency of surface algae blooms in a drinking water reservoir. Using the techniques utilized in this study may allow for the application of rapid-response systems during the onset of seasonal algal blooms. We recommend that future studies investigate different remote sensing datasets and combine them with in-situ data measurements to evaluate the accuracy of the proposed approach and show clearly the relationship between different types of algae blooms and the water surface changes in spectral reflectance.

Authors contribution

Tarq K.Hassan conceived and designed the experiment. Haidi Abdullah analyzed the data and wrote the manuscript. All authors contributed to editing of the manuscript.

Conflict of intrestrst

The authors declare no conflict of interest.

Reference

Alawadi, F. 2010. Detection of surface algal blooms using the newly developed algorithm surface algal bloom index (SABI). Remote Sensing of the Ocean, Sea Ice, and Large Water Regions 2010, International Society for Optics and Photonics.

Bresciani, M., Giardino, C., Lauceri, R., Matta, E., Cazzaniga, I., Pinardi, M., Lami, A., Austoni, M., Viaggiu, E. and Congestri, R. 2017. Earth observation for monitoring and mapping of cyanobacteria blooms. Case studies on five Italian lakes."

Chorus, I. and Bartram, J. 1999. Toxic cyanobacteria in water: a guide to their public health consequences, monitoring and management, CRC Press.

Codd, G. A., Lindsay, Young, J. F. M., Morrison, L. F. and Metcalf, J.S. 2005. Harmful cyanobacteria. *Harmful Cyanobacteria,* Springer**:** 1-23.

Cook, C. and Bakker, K. 2012. Water security: Debating an emerging paradigm. *Global Environmental Change* 22(1) : 94-102.

Doxaran, D., Froidefond, J. M. and Castaing, P. 2002. A reflectance band ratio used to estimate suspended matter concentrations in sediment-dominated coastal waters. *International Journal of Remote Sensing.* 23(23) : 5079-5085.

Hestir, E. L., Brando, V. E., Bresciani, M., Giardino, C., Matta, E., Villa, P. and Dekker, A. G. 2015. Measuring freshwater aquatic ecosystems: The need for a hyperspectral global mapping satellite mission. *Remote Sensing of Environment.* 167 : 181-195.

Hu, C., Lee, Z., Ma, R., Yu, K., Li, D. and Shang, S. 2010. Moderate resolution imaging spectroradiometer (MODIS) observations of cyanobacteria blooms in Taihu Lake, China. *Journal of Geophysical Research: Oceans.* 115(C4).

Keith, D. 2010. Estimating chlorophyll conditions in southern New England coastal waters from hyperspectral remote sensing. *Remote Sensing of Coastal Environments. CRC Press, Boca Raton, Florida.* 151-172.

Klemas, V. 2012. Remote sensing of algal blooms: an overview with case studies. *Journal of Coastal Research.* 28(1A) : 34-43.

Ogashawara, I., Li, L. and Moreno-Madriñán, M. J. 2016. Slope algorithm to map algal blooms in inland waters for Landsat 8/Operational Land Imager images. *Journal of Applied Remote Sensing.* 11(1) : 012005.

Paerl, H. W. 1996. A comparison of cyanobacterial bloom dynamics in freshwater, estuarine and marine environments. *Phycologia.* 35(sup6): 25-35.

Pilesjo, P. and Al-Juboori, S. S. 2016. Modelling the effects of climate change on hydroelectric power in Dokan, Iraq. *Int. J. Energy Power Eng.* 5(2): 7.

Reynolds, C. 1990. Temporal scales of variability in pelagic environments and the response of phytoplankton. *Freshwater Biology.* **23** (1): 25-53.

Schalles, J. F., Gitelson, A. A., Yacobi, Y. Z. and Kroenke, A. E. 1998. Estimation of chlorophyll a from time series measurements of high spectral resolution reflectance in an eutrophic lake. *Journal of Phycology.* 34(2) : 383-390.

Setty, K., Jiménez, A., Willetts, J., Leifels, M. and Bartram, J. 2020. Global water, sanitation and hygiene research priorities and learning challenges under Sustainable Development Goal 6. *Development Policy Review.* 38(1) : 64-84.

Toma, J. J. 2019. Algae as indicator to assess trophic status in Dokan Lake, Kurdistan region of Iraq. *Zanco Journal of Pure and Applied Sciences.* 31(2) : 57-64.

Vaux, J. H. 2001. Water Quality (Book Review). *Environment.* 43(3) : 39-39.

Vincent, W. F., L. G. Whyte, C. Lovejoy, C. W. Greer, I. Laurion, C. A. Suttle, J. Corbeil and D. R. Mueller 2009. Arctic microbial ecosystems and impacts of extreme warming during the International Polar Year. *Polar Science.* **3**(3): 171-180.